



Asteroseismology of HD 129929: Core Overshooting and Nonrigid Rotation

C. Aerts, *et al.*

Science **300**, 1926 (2003);

DOI: 10.1126/science.1084993

The following resources related to this article are available online at www.sciencemag.org (this information is current as of May 16, 2008):

Updated information and services, including high-resolution figures, can be found in the online version of this article at:

<http://www.sciencemag.org/cgi/content/full/300/5627/1926>

Supporting Online Material can be found at:

<http://www.sciencemag.org/cgi/content/full/1084993/DC1>

A list of selected additional articles on the Science Web sites **related to this article** can be found at:

<http://www.sciencemag.org/cgi/content/full/300/5627/1926#related-content>

This article has been **cited by** 40 article(s) on the ISI Web of Science.

This article appears in the following **subject collections**:

Astronomy

<http://www.sciencemag.org/cgi/collection/astronomy>

Information about obtaining **reprints** of this article or about obtaining **permission to reproduce this article** in whole or in part can be found at:

<http://www.sciencemag.org/about/permissions.dtl>

number of potential positions along the inner helix allow bending.

It is possible that the channel makes use of both Gly¹³⁴ and Gly¹⁴³ sites during gating, but we believe that Gly¹³⁴ plays a minor role in gating and a more important role in protein packing in Kir channels. Hence, as the channel begins to open, the slide helix moves laterally. Strain is exerted on the bottom of the inner helix, resulting in distortion of the helix at the nearest weak point, Gly¹⁴³. The blocking residue side chain of Phe¹⁴⁶ beneath Gly¹⁴³ then moves away from the center of the ion-conduction pathway.

Coupling of gating domain to the blocking residue. All ion channels have an ion-conduction pathway and a gate. Features of the ion-conduction pathway determine the specificity and rate of ion conduction, whereas the gate functions as a switch, opening and closing the pore at the desired time. The section of the protein that detects a signal such as a change in voltage across the membrane or binding of a ligand must transmit the signal to the gate to produce a gating action. With KirBac1.1 there has to be a coupling mechanism between the blocking residues of the inner helices and the intracellular domains.

The amphipathic slide helix is well placed to play a central role in this coupling mechanism. When the C-terminal assembly receives a signal, it is likely to undergo a conformational change. Again the precise change is unknown, but a rotation centered within the C-terminal domain would be consistent with the KirBac1.1 model and the proposed MthK domain motion. Because the outer helix is directly connected to the slide helix, it must move in the same

direction, thereby creating room for the inner helix to bend.

Summary. KirBac1.1 was crystallized in a closed state, whereas all other K⁺ channel structures to date have been open. KirBac1.1 prevents ion conduction by (i) occluding the ion-conduction pathway with the use of hydrophobic phenylalanine side chains, (ii) misaligning pore helices, (iii) decreasing the volume of the central cavity, and (iv) altering the conformation of the selectivity filter. The structure provides a hypothesis for gating, involving intracellular domain movement, slide helix movement, and bending of the inner helix just above the blocking residue. In our view, many K⁺ channels are likely to share a fundamentally similar mechanism of gating and coupling in which properties of the gating domains determine how and when the channel opens.

References and Notes

1. F. M. Ashcroft, *Ion Channels and Diseases* (Academic Press, New York, 2000).
2. B. Hille, *Ionic Channels of Excitable Membranes* (Sinauer, Sunderland, MA, 2001).
3. S. R. Durell, H. R. Guy, *BMC Evol. Biol.* **1**, 14 (2001).
4. Materials and Methods are available as supporting material on Science Online.
5. M. Nishida, R. MacKinnon, *Cell* **111**, 957 (2002).
6. D. A. Doyle et al., *Science* **280**, 69 (1998).
7. D. M. Cortes, L. G. Cuello, E. Perozo, *J. Gen. Physiol.* **117**, 165 (2001).
8. D. L. Minor Jr., S. J. Masseling, Y. N. Jan, L. Y. Jan, *Cell* **96**, 879 (1999).
9. G. Loussouarn, E. N. Makhina, T. Rose, C. G. Nichols, *J. Biol. Chem.* **275**, 1137 (2000).
10. Z. Lu, R. MacKinnon, *Nature* **371**, 243 (1994).
11. B. A. Wible, M. Tagliatela, E. Ficker, A. M. Brown, *Nature* **371**, 246 (1994).
12. Y. Kubo, Y. Murata, *J. Physiol.* **531** (no. 3), 645 (2001).
13. J. Yang, Y. N. Jan, L. Y. Jan, *Neuron* **14**, 1047 (1995).
14. M. Tagliatela, E. Ficker, B. A. Wible, A. M. Brown, *EMBO J.* **14**, 5532 (1995).
15. K. Imoto et al., *Nature* **335**, 645 (1988).
16. A. N. Lopatin, E. N. Makhina, C. G. Nichols, *Nature* **372**, 366 (1994).
17. B. Fakler et al., *FEBS Lett.* **356**, 199 (1994).
18. E. Ficker, M. Tagliatela, B. A. Wible, C. M. Henley, A. M. Brown, *Science* **266**, 1068 (1994).
19. S.-C. Tam, R. J. P. Williams, *J. Chem. Soc., Faraday Trans. 1* **80**, 2255 (1983).
20. N. Unwin, *J. Mol. Biol.* **229**, 1101 (1993).
21. N. Unwin, *Nature* **373**, 37 (1995).
22. G. Chang, R. H. Spencer, A. T. Lee, M. T. Barclay, D. C. Rees, *Science* **282**, 2220 (1998).
23. O. Beckstein, P. C. Biggins, M. S. P. Sansom, *J. Phys. Chem. B* **105**, 12902 (2001).
24. B. Roux, R. MacKinnon, *Science* **285**, 100 (1999).
25. Y. Zhou, J. Morais-Cabral, A. Kaufman, R. MacKinnon, *Nature* **414**, 43 (2001).
26. J. N. Bright, I. H. Shrivastava, F. S. Cordes, M. S. P. Sansom, *Biopolymers* **64**, 303 (2002).
27. Y. Jiang et al., *Nature* **417**, 523 (2002).
28. D. del Camino, M. Holmgren, Y. Liu, G. Yellen, *Nature* **403**, 321 (2000).
29. Aesop; M. E. M. Noble, University of Oxford.
30. We thank the staff of the European Synchrotron Radiation Facility for help with data collection, including E. Gordon, J. McCarthy, S. Monaco, and S. Kozielski. D.A.D. is grateful for support and helpful discussions from L. Johnson, M. Sansom, B. Guy, B. Wallace, L. Hong, S. Iwata, and M. Noble. J.M.G. thanks P. Colman and B. Smith. F.M.A. is funded by the Wellcome Trust and Medical Research Council. J.M.G. was funded by an International Senior Fellowship of the Wellcome Trust and by Australian National Health and Medical Research Council grant 257528. This work was funded by a Wellcome Trust Research Career Development Fellowship awarded to D.A.D. Coordinates for the KirBac1.1 structure have been deposited with the Protein Data Bank (accession code 1P7B; ID no. RCSB019097).

Supporting Online Material

www.sciencemag.org/cgi/content/full/1085028/DC1
Materials and Methods
Figs. S1 and S2
References

27 March 2003; accepted 29 April 2003
Published online 8 May 2003;
10.1126/science.1085028
Include this information when citing this paper.

REPORTS

Asteroseismology of HD 129929: Core Overshooting and Nonrigid Rotation

C. Aerts,^{1*} A. Thoul,² J. Daszyńska,^{1,3} R. Scuflaire,² C. Waelkens,¹ M. A. Dupret,² E. Niemczura,³ A. Noels²

We have gathered and analyzed 1493 high-quality multicolor Geneva photometric data taken over 21 years of the B3V star HD 129929. We detect six frequencies, among which appear the effects of rotational splitting with a spacing of ~ 0.0121 cycles per day, which implies that the star rotates very slowly. A nonadiabatic analysis of the oscillations allows us to constrain the metallicity of the star to $Z \in [0.017, 0.022]$, which agrees with a similar range derived from spectroscopic data. We provide evidence for the occurrence of core convective overshooting in the star, with $\alpha_{ov} = 0.10 \pm 0.05$, and we rule out rigid rotation.

Stars are composed of multiple gas layers with different temperatures, pressures, and chemical compositions. During their main-

sequence phase, that is, while they transform hydrogen into helium in their core, a number of massive stars undergo oscillations.

Through the study of these oscillations, scientists have a unique opportunity to probe the structure of specific layers of those stars. This type of investigation is termed asteroseismology. Here, we used asteroseismology to study the interior structure of a 10-solar mass (M_{\odot}) star of spectral type B, HD 129929. Such a massive B star has a well-developed convective core, the extension of which is uncertain because it depends on a poorly known phenomenon called core overshooting (inertial mixing of material from the convective core to the convectively stable upper layer). Moreover, the rotation of the star may be a source of mixing between the core and the outer layers. Both effects, which are in general difficult to disentangle from each other (*1*), affect the evolutionary path of the star; that is, they determine the way in which the star evolves to its supernova stage. In the case of HD 129929, we sought to determine the ef-

fectiveness of the overshooting phenomenon, technically measured by the overshooting parameter (α_{ov}).

Oscillating main-sequence B stars more massive than 8 solar masses are called β -Cephei variables. Their individual oscillation modes, which are driven by an opacity mechanism acting in the metal opacity bump at a temperature of some 200,000°C (2), have multiple periods between 2 and 8 hours. This condition leads to beat periods on the order of several months, which is much longer than the beat periods of main-sequence stars that exhibit solarlike oscillations or of the oscillations in compact stars such as white dwarfs. Moreover, the oscillation frequencies in solarlike stars and in white dwarfs are more numerous and obey certain regular patterns (3, 4), which makes their modes much easier to identify than opacity-driven modes in massive stars. This is one of the reasons that

seismic studies of solarlike stars and of white dwarfs are much further advanced than are those of opacity-driven oscillators.

HD 129929 (visual magnitude 8.1, spectral type B3V) was discovered to be a microvariable (5). Three close frequencies were established (6, 7) in multicolor photometry of the star, which led (6) to classification of the object as a new β -Cephei star. We have continued the photometric monitoring of the star and have assembled 1493 high-quality (error < 5 millimagnitudes) multicolor data points during several 3-week runs throughout 21.2 years. All data were gathered with the seven-passband Geneva photometer P 7 attached to the 0.7-m Swiss telescope at La Silla Observatory in Chile. The effective temperature and the gravity of HD 129929 are available from calibrations of photometric systems (8, 9). These parameters and the metallicity of the star were also derived from low-resolution spectra taken with the International Ultraviolet Explorer (10). The overall range in quoted values of the temperature and gravity is, respectively, $\log T_{\text{eff}} \in [4.35, 4.38]$ and $\log g \in [3.87, 3.94]$, and the metallicity is $Z = 0.018 \pm 0.004$ (10). We have used these estimates as the starting point of our model grid calculations, but we stress that

our modeling results are independent of this particular result. In fact, we considerably improve the estimates of the temperature and the gravity with our seismic analysis.

We have performed both phase dispersion minimization (11) and Fourier analysis (12) on the time series of 1493 data points in each of the seven Geneva filters (Fig. 1). The six frequencies that result were found by both of these independent techniques, and all six frequencies are found independently of the order of prewhitening (i.e., subsequent sine curve subtraction). The periodograms (Fig. 1 and Table 1) show that $f_1 - f_3 \cong f_2 - f_6 \cong f_4 - f_2 \cong 0.0121$ cycles per day (c d^{-1}); i.e., two frequency multiplets due to rotational splitting appear in the data. We note that the highest peaks in the periodograms do not occur for f_5 and f_6 but for their 1-day alias (Fig. 1). We can be sure of this both for physical reasons and for reasons related to our models. All models that obey f_1, \dots, f_6 do not lead to a low-degree mode at $f_5 - 1$ or any other alias of f_5 , whereas they result in the radial fundamental mode at f_5 . Similarly, there is no low-degree mode available near $f_6 + 1$, whereas f_6 corresponds to the $l = 1, p_1$ mode shifted by the rotation. The frequencies that show up after prewhitening with f_1, \dots, f_6 no longer coincide for the different Geneva filters and/or for the different analysis methods. We hence regard them as ambiguous, and we only make use of the six established frequencies (Fig. 2), which consist of one isolated frequency and (parts of) two multiplets.

We modeled the interior structure of HD 129929 with two independent evolutionary codes, namely the Code Liégeois d'Évolution Stellaire (13) and the Warsaw–New Jersey Evolutionary Code (14). We have considered a large range in $\log T_{\text{eff}}$ and in $\log g$ and allowed $X \in [0.68, 0.74]$, $Y \in [0.24, 0.3]$, and $Z \in [0.015, 0.03]$. We used the opacities derived from the OPAL code (15), completed with the Alexander and Ferguson opacities (16) below $\log T = 3.95$ and the standard heavy-element mixture (17). For all these models, we have calculated the oscillation modes with two independent codes for linear nonadiabatic oscillations (18, 19). All the results obtained from these independent codes

¹Instituut voor Sterrenkunde, Katholieke Universiteit Leuven, Celestijnenlaan 200 B, B-3001 Leuven, Belgium. ²Institut d'Astrophysique et Géophysique, Université de Liège, allée du Six Août 17, B-4000 Liège, Belgium. ³Astronomical Institute of the Wrocław University, ul. Kopernika 11, 51-622 Wrocław, Poland.

*To whom correspondence should be addressed. E-mail: conny@ster.kuleuven.ac.be

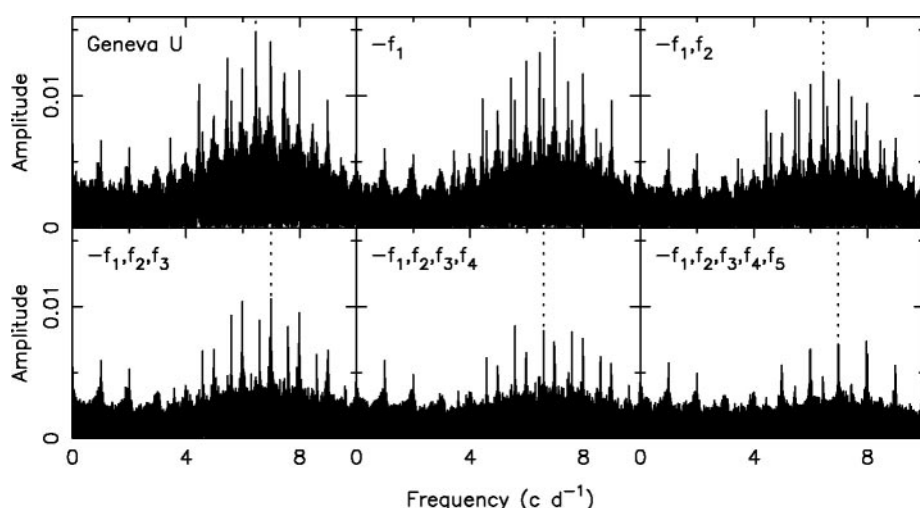


Fig. 1. Periodograms for the Geneva U data for subsequent stages of prewhitening. The amplitude is expressed in magnitudes. For the values of the frequencies, refer to Table 1. The dotted lines indicate the selected frequencies.

Table 1. Accepted frequencies f_i , $i = 1, \dots, 6$ for HD 129929. The standard error is less than 10^{-6} c d^{-1} (cycles per day) for all listed frequencies. l and m denote the degree and the azimuthal number of the oscillation modes. The amplitudes are expressed in millimagnitudes.

Oscillation frequencies (c d^{-1})	Amplitude (in U)	Amplitude (in V)	Mode identification	Frequency splitting (c d^{-1})
$f_1 = 6.461699$	14.7 ± 0.6	11.8 ± 0.4	$l = 2, m = ?, g_1$	
$f_2 = 6.978305$	14.9 ± 0.8	10.3 ± 0.5	$l = 1, m = 0, p_1$	
$f_3 = 6.449590$	11.7 ± 0.6	9.1 ± 0.4	$l = 2, m = ?, g_1$	
$f_4 = 6.990431$	11.6 ± 0.8	7.5 ± 0.5	$l = 1, m = +1, p_1$	$f_1 - f_3 = 0.012109$
$f_5 = 6.590940$	9.4 ± 0.8	4.9 ± 0.5	$l = 0, m = 0, p_1$	$f_4 - f_2 = 0.012126$
$f_6 = 6.966172$	7.6 ± 0.6	4.8 ± 0.5	$l = 1, m = -1, p_1$	$f_2 - f_6 = 0.012133$

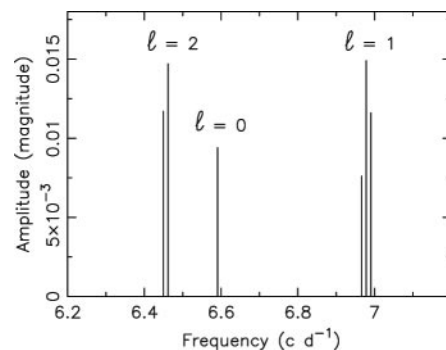


Fig. 2. Final amplitude spectrum of HD 129929.

REPORTS

are the same to a high degree of accuracy.

The second step in a seismic analysis consists of mode identification of the detected frequencies, that is, to derive the wave numbers (n, l, m) of the modes. The degree l of the modes can be derived from the amplitude ratios and phase differences of multi-color photometry. We have used the two nonadiabatic oscillation codes (18, 19) to do so and found agreement for the identifications (Table 1). These identifications are unambiguous because of the sparse frequency distribution due to the slow rotation of HD 129929. Following (20, 21), who provided a method to derive constraints on the metallicity of the star from the observed amplitude ratios in B stars, we find that $Z < 0.022$ is needed to meet the observed amplitudes and their errors. Moreover, for $Z < 0.017$, the modes corresponding to the observed frequencies are not excited by the opacity mechanism. This seismically determined interval $Z \in [0.017, 0.022]$ is consistent with the one derived from the independent spectroscopic observations. The physical behavior of the modes of HD 129929 (fig. S2) is representative of the nature of the propagation zone in which they are trapped.

We have computed numerous stellar models, and only a few of them lead to the observed frequencies f_5 and f_2 , which correspond to the radial and axisymmetric dipole modes—modes that are unaffected by the rotation of the star (fig. S3). For all the models that explain f_5 and f_2 well, we have also calculated the frequency of the $l = 2$, g_1 axisymmetric mode and compared its value with the possible values for that mode for the case $X = 0.7$ (Fig. 3, left). We conclude that the overshooting parameter α_{ov} cannot be equal to 0.2, because this results in a value for the frequency of the $l = 2$ axisymmetric mode that is too small. Similarly, it cannot be

0, because this value gives results that are inconsistent with the photometric amplitude ratios. The value $\alpha_{ov} = 0.1$ is, on the other hand, totally acceptable, and for this value we derive $M \in [9, 9.5] M_\odot$ (Fig. 3, right). The same results are obtained for models with other values of the parameter $X \in [0.68, 0.74]$. The corresponding ages of the allowed models are between 1.6×10^7 and 1.8×10^7 years. These models are situated between those indicated by arrows in fig. S3.

The observation of the triplet of frequencies (f_6, f_2, f_4) of the $l = 1, p_1$ mode and of the two components (f_3, f_1) of the quintuplet of the $l = 2, g_1$ mode (Fig. 2) also allows us to determine the rotation frequency of the star. The rotational splitting Δf is linked to the internal rate of rotation of the star ν_{rot} through the linear relation $\Delta f = \int K_{nl}(r) \nu_{rot}(r) dr$, where the kernel $K_{nl}(r)$ is completely defined by the mode identification and by the stellar model. The observed splittings $\Delta f = 0.0121295 \text{ c d}^{-1}$ for the $l = 1, p_1$ mode and $\Delta f = 0.012109 \text{ c d}^{-1}$ for the $l = 2, g_1$ mode are incompatible with a rigid rotation of the star for the accepted stellar models. Indeed, the first one would imply $\nu_{rot} = 0.012653 \text{ c d}^{-1}$, whereas the second one would imply $\nu_{rot} = 0.014730 \text{ c d}^{-1}$. On the other hand, both modes have amplitudes that are too low in the inner regions of the star to give any information on the rotation inside the core. To estimate the rotational behavior in the outer layers, we have assumed the behavior of ν_{rot} to follow a linear law of the form $\nu_{rot}(r) = \nu_{rot,0} + (r/R - 1)\nu_{rot,1}$. We then get $\nu_{rot,0} = 0.00713 \text{ c d}^{-1}$ and $\nu_{rot,1} = -0.01856 \text{ c d}^{-1}$. These values imply a low equatorial rotation velocity of 2.04 km s^{-1} .

We note that no model calculation from the Opacity Project (OP) tables (22) leads to the observed frequencies for appropriate ranges in the stellar parameters of HD

129929. It is at present unclear whether this is due to the 2.5% higher iron fraction or to the different physics used to calculate the OP tables in comparison with the OPAL tables.

Convective core overshooting is not considered in some evolutionary model calculations of massive main-sequence stars (23). The reason is that it does not seem to be a necessary ingredient to explain the observed properties of such stars. However, we have found evidence for the presence of overshooting with $\alpha_{ov} \in [0.05, 0.15]$ in HD 129929, because the star has an extremely low rotational velocity, so rotational effects can be neglected. We have adopted the standard solar mixture in our model calculations; an important open question, for any asteroseismic analysis, is how much the results may change if a different mixture is considered.

References and Notes

1. J.-C. Mermilliod, A. Maeder, *Astron. Astrophys.* **158**, 45 (1986).
2. W. A. Dziembowski, A. A. Pamyatnykh, *Astron. Astrophys.* **248**, L11 (1993).
3. F. Bouchy, F. Carrier, *Astron. Astrophys.* **374**, L5 (2001).
4. D. E. Winget et al., *Astrophys. J.* **378**, 326 (1991).
5. F. Rufener, *Astron. Astrophys. Suppl. Ser.* **45**, 207 (1981).
6. C. Waelkens, F. Rufener, *Astron. Astrophys.* **119**, 279 (1983).
7. D. Heynderickx, *Astron. Astrophys. Suppl. Ser.* **96**, 207 (1992).
8. R. R. Shobbrook, *Mon. Not. R. Astron. Soc.* **214**, 33 (1985).
9. D. Heynderickx, C. Waelkens, P. Smeyers, *Astron. Astrophys.* **105**, 447 (1994).
10. J. Daszyńska, E. Niemczura, in preparation.
11. R. F. Stellingwerf, *Astrophys. J.* **224**, 953 (1978).
12. J. D. Scargle, *Astrophys. J.* **263**, 835 (1982).
13. R. Scuflaire, in preparation.
14. B. Paczyński, *Acta Astron.* **20**, 47 (1970).
15. F. J. Rogers, C. A. Iglesias, *Astrophys. J.* **401**, 361 (1992).
16. D. R. Alexander, J. W. Ferguson, *Astrophys. J.* **437**, 879 (1994).
17. N. Grevesse, A. Noels, in *Origin and Evolution of the Elements*, N. Pratz, E. Vangioni, M. Casse, Eds. (Cambridge Univ. Press, Cambridge, 1993), pp. 15–25.
18. W. A. Dziembowski, *Acta Astron.* **27**, 95 (1977).
19. M.-A. Dupret, *Astron. Astrophys.* **366**, 166 (2001).
20. M.-A. Dupret et al., *Astron. Astrophys.* **398**, 677 (2003).
21. M.-A. Dupret et al., *Astron. Astrophys.* **385**, 563 (2002).
22. M. J. Seaton, *Mon. Not. R. Astron. Soc.* **279**, 95 (1996).
23. A. Pamyatnykh, *Acta Astron.* **49**, 119 (1999).
24. We are indebted to all the researchers from Leuven and Geneva who contributed to the gathering of the data over the course of 21 years. C.A. and C.W. acknowledge financial support from the Fund for Scientific Research of Flanders (FWO). A.T., R.S., M.A.D., and A.N. acknowledge financial support from the Interuniversity Attraction Pole (IAP, Belgium), from Programme de Développement d'Expériences Scientifiques (PRODEX) of the European Space Agency, and from the Fonds pour la Formation à la Recherche dans l'Industrie et dans l'Agriculture (FRIA, Belgium). A.T. acknowledges financial support from the Fonds National de la Recherche Scientifique (FNRS, Belgium). J.D. acknowledges financial support from the Belgian Federal Office for Scientific, Technical, and Cultural Affairs (OSTC, Belgium).

Supporting Online Material

www.sciencemag.org/cgi/content/full/1084993/DC1
Figs. S1 to S3

27 March 2003; accepted 14 May 2003

Published online 29 May 2003;

10.1126/science.1084993

Include this information when citing this paper.

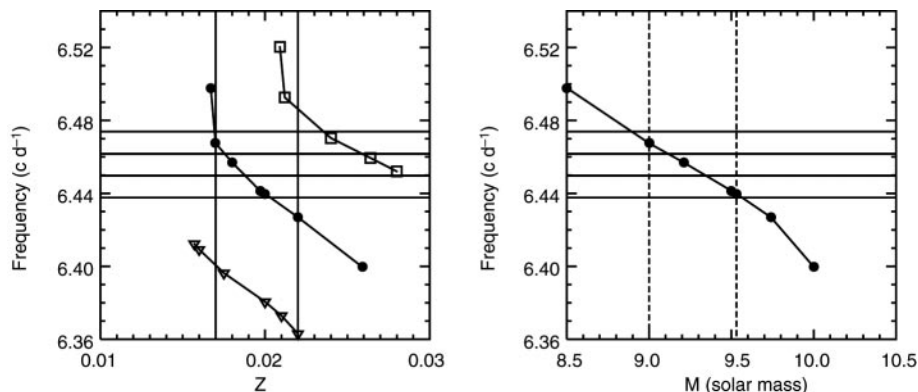


Fig. 3. Frequency of the $l = 2$ axisymmetric mode for the models with $X = 0.7$ that fit the frequencies f_5 and f_2 . The squares, dots, and triangles are obtained for $\alpha_{ov} = 0, 0.1$, and 0.2 , respectively. The four horizontal lines are the possible values derived from the observations for this axisymmetric mode. (Left) Frequency as a function of metallicity Z . The seismic constraints on Z are represented as vertical lines. (Right) Frequency as a function of mass M for models with $\alpha_{ov} = 0.1$. The constraints on the mass obtained by imposing $0.017 < Z < 0.022$ and by requiring that the $l = 2$ frequency be consistent with the observations are represented as dashed vertical lines.